NeuroToxicology 56 (2016) 76–85

Contents lists available at ScienceDirect

NeuroToxicology

Full length article

Synergy as a new and sensitive marker of basal ganglia dysfunction: A study of asymptomatic welders

Mechelle M. Lewis[a,b], Eun-Young Lee[a], Hang Jin Jo[f], Guangwei Du[a], Jaebum Park[g], Michael R. Flynn[h], Lan Kong[e], Mark L. Latash[f,**], Xuemei Huang[a,b,c,d,f,*]

[a] Department of Neurology, Pennsylvania State University-Milton S. Hershey Medical Center, Hershey, PA 17033, United States
[b] Department of Pharmacology, Pennsylvania State University-Milton S. Hershey Medical Center, Hershey, PA 17033, United States
[c] Department of Radiology, Pennsylvania State University-Milton S. Hershey Medical Center, Hershey, PA 17033, United States
[d] Department of Neurosurgery, Pennsylvania State University-Milton S. Hershey Medical Center, Hershey, PA 17033, United States
[e] Department of Biostatistics, Pennsylvania State University-Milton S. Hershey Medical Center, Hershey, PA 17033, United States
[f] Department of Kinesiology, The Pennsylvania State University, University Park, PA 16802, United States
[g] Institute of Sport Science, Seoul National University, Seoul, South Korea
[h] Department of Environmental Sciences and Engineering, Gillings School of Global Public Health, University of North Carolina, Chapel Hill, NC, United States

ARTICLE INFO

Article history:
Received 9 May 2016
Received in revised form 20 June 2016
Accepted 29 June 2016
Available online 30 June 2016

Keywords:
Synergy
MRI
Welders
Low-level exposure
Basal ganglia

ABSTRACT

Background: Multi-digit synergies, a recently developed, theory-based method to quantify stability of motor action, are shown to reflect basal ganglia dysfunction associated with parkinsonian syndromes. In this study, we tested the hypothesis that multi-digit synergies may capture early and subclinical basal ganglia dysfunction. We chose asymptomatic welders to test the hypothesis because the basal ganglia are known to be most susceptible to neurotoxicity caused by welding-related metal accumulation (such as manganese and iron).

Methods: Twenty right-handed welders and 13 matched controls were invited to perform single- and multi-finger pressing tasks using the fingers of the right or left hand. Unified Parkinson's Disease Rating Scale and Grooved Pegboard scores were used to gauge gross and fine motor dysfunction, respectively. High-resolution (3T) T1-weighted, T2-weighted, T1 mapping, susceptibility, and diffusion tensor MRIs were obtained to reflect manganese, iron accumulation, and microstructural changes in basal ganglia. The synergy index stabilizing total force and anticipatory synergy adjustments were computed, compared between groups, and correlated with estimates of basal ganglia manganese [the pallidal index, R1 (1/T1)], iron [R2* (1/T2*)], and microstructural changes [fractional anisotropy and mean diffusivity].

Results: There were no significant differences in Unified Parkinson's Disease Rating Scale (total or motor subscale) or Grooved Pegboard test scores between welders and controls. The synergy index during steady-state accurate force production was decreased significantly in the left hand of welders compared to controls ($p = 0.004$) but did not reach statistical significance in the right hand ($p = 0.16$). Anticipatory synergy adjustments, however, were not significantly different between groups. Among welders, higher synergy indices in the left hand were associated significantly with higher fractional anisotropy values in the left globus pallidus ($R = 0.731$, $p < 0.001$) but not with the pallidal index, R1, or R2* values in the basal ganglia.

Conclusions: These data suggest that multi-digit synergy metrics may serve as preclinical markers for basal ganglia dysfunction in welders and other populations at risk for neurodegenerative diseases involving parkinsonian symptoms. This finding may have important clinical, scientific, and public/occupational health implications.

1. Introduction

Since all natural human movements are performed in a poorly predictable environment and involve varying internal states, movement stability is crucial for successful everyday motor performance. For example, holding a cup of water steady requires

* Corresponding author at: Departments of Neurology, Neurosurgery, Radiology, Pharmacology, and Kinesiology, Penn State University—Milton S. Hershey Medical Center, 500 University Drive, H037, Hershey, PA 17033-0850, United States.
** Corresponding author at: Department of Kinesiology, Rec Hall 268N, The Pennsylvania State University, University Park, PA 16802, United States.
E-mail addresses: mll11@psu.edu (M.L. Latash), Xuemei@psu.edu (X. Huang).

http://dx.doi.org/10.1016/j.neuro.2016.06.016
0161-813X/

stability of the integrated contribution of the many involved joints and muscles, all of which may vary their state. It is important to note that stability is not always desirable. If a person wants to make a quick action, high stability would resist this intentional change. We address the ability to modify steady states in preparation to a quick action as agility. Loss of stability of motor performance may cause spills, falls (balance problems), dropped objects, illegible writing, stuttering, etc., whereas loss of agility may cause difficulty in motor initiation (such as freezing of gait). These examples are extreme and obvious; but loss of movement stability also may be subtle and not observable with the naked eye.

Until recently, no method could quantify movement stability of motor function across the repertoire of everyday actions that involve multi-digit object manipulation, multi-joint reaching, and whole-body actions. Based on two theoretical constructs, the principle of abundance (Gelfand and Latash, 1998; Latash, 2012) and the uncontrolled manifold hypothesis (Scholz and Schoner, 1999), we have developed an index of motor synergies ensuring action stability. We define synergies as task-specific organizations of redundant (abundant, Latash, 2012) sets of elements. All human movements involve abundant sets of elements; as a result, a given value of a performance variable (e.g., total force produced by a set of fingers) can be achieved with numerous combinations of elemental variables (e.g., finger forces). If a person performs several task trials, elemental variables are expected to diverge in less stable directions and converge in more stable directions. As a result, stabilizing a salient performance variable (such as total force) may be expected to lead to relatively high inter-trial variance of elemental variables within the sub-space where the performance variable does not change (its uncontrolled manifold, UCM; Scholz and Schoner, 1999) compared to variance orthogonal to the UCM direction, ORT. Variance along the UCM (V_{UCM}) has no effect on the performance variable, as it reflects flexible use of varying solutions to ensure the same performance across slightly changing effector (e.g., finger) contributions. Variance along the ORT (V_{ORT}) reflects accuracy of performance. The normalized difference between V_{UCM} and V_{ORT} has been defined as a synergy index (ΔV; reviewed in Latash et al., 2002, 2007). Prior to a quick change in the corresponding performance variable, a drop in an index of stability was observed in young, healthy persons 200–300 ms prior to the initiation of a quick action from steady state (Olafsdottir et al., 2005). We defined this phenomenon as anticipatory synergy adjustments (ASAs), which reflect the ability to modify a steady state in experimental studies.

As a new concept (Latash and Huang, 2015), the syndrome of impaired control of stability has not been mentioned in clinics or human health-related research. Currently, the main test of basal ganglia dysfunction in a clinical setting is the Unified Parkinson's Disease (PD) Rating Scale (UPDRS). The scale is subjective, offers little insight into motor coordination, and is not useful in asymptomatic populations with subclinical basal ganglia dysfunction. The Grooved Pegboard test also has been used for gauging fine motor dysfunction (reviewed in Ruff and Parker, 1993; Causby et al., 2014). This test may be useful and sensitive to detect definite declines in fine motor skills for patient populations (Lee et al., 2013) but may not be sensitive to detect subtle motor function changes in subclinical populations (Ellingsen et al., 2008).

Recently, we demonstrated that perturbation of the basal ganglia in PD and parkinsonism patients leads to a significant decrease in synergy indices and ASAs (Park et al., 2012; Park et al., 2013b; Jo et al., 2015), suggesting impairments both in creating task-specific stability of salient variables (cf. Schöner, 1995) and adjusting it in anticipation of a quick action. Most importantly, we found synergy changes in early-stage PD patients, even in the asymptomatic limb. Together, these data suggested that multi-digit synergies might capture subclinical basal ganglia dysfunction. Testing this hypothesis is important because many neurodegenerative disorders have a long pre-clinical period (Sandberg et al., 2001; Mandel and Korczyn, 2011; Eisen et al., 2014) and developing tests that sensitively detect preclinical signs also may help develop neuroprotective methods.

Overt Mn neurotoxicity is known to have similarities to PD (Cersosimo and Koller, 2006; Bowler et al., 2007a). The neurotoxic effects of chronic and lower-level Mn exposure, at the level most relevant to occupational and public health, however, are less clear. Asymptomatic welders with relatively low exposure levels may serve as a human model of subclinical basal ganglia dysfunction based on the following knowledge: 1) High-exposure welding causes a clinical syndrome similar to PD (manganese-induced parkinsonism or manganism) such as slowness of movements, tremor, and balance problems. Their symptoms, however, are probably related to excessive exposure to manganese (Mn) (Huang et al., 1993; Hauser et al., 1996; Mergler and Baldwin, 1997; Pal et al., 1999; Guilarte, 2013), although our group has demonstrated recently that higher accumulation of iron also occurs in welders (Lee et al., 2016b). 2) Many studies have documented subclinical symptoms (e.g., declines in neuropsychological or motor performance) that do not meet criteria for overt manganism (Bowler et al., 2006a,b; Bowler et al., 2007a,b; Ellingsen et al., 2008; Chang et al., 2009; Cowan et al., 2009a,b; Simon-Sanchez et al., 2009). 3) Although manganism can be differentiated from PD by the lack of L-dopa response (Ostiguy et al., 2006), they share the common feature of basal ganglia dysfunction. In PD, the basal ganglia dysfunction arises from dopaminergic cell loss in the substantia nigra, whereas in manganism it may be related to Mn accumulation in the basal ganglia, especially in the globus pallidus (Kim et al., 1999; Dorman et al., 2006; Criswell et al., 2012; Lee et al., 2015, 2016b). Thus, asymptomatic welders with relatively low exposure levels may represent a transitional group that allows us to determine if synergy metrics can serve as a sensitive measurement for preclinical basal ganglia dysfunction.

In this study, we tested the following two hypotheses: 1) multi-digit synergy and ASA indices in welders are reduced compared to controls; 2) reduced synergy metrics in welders are associated with exposure measurements (welding-related metal accumulation and/or microstructural changes) in the basal ganglia.

2. Materials and methods

2.1. Subjects

Twenty welders and 13 matched controls were selected from a larger cohort of subjects in an exposure and neuroimaging study. The original cohort of 80 subjects (40 welders and 40 controls) was recruited from regional union meetings in central PA, USA, and from the community around the Penn State Hershey Medical Center (PSHMC; Lee et al., 2015). Welders were defined as subjects who had welded at any point in their lifetime and controls as those who did not have any history of welding. Subjects selected for this study were all male, right-handed according to their preferred hand during writing and eating, and answered negatively for past diagnosis of neurological disorders. As part of the screening visit, detailed demographic information was obtained from all subjects. Since all subjects in the overall cohort were male, matching by gender was not an issue for the current study. We attempted to match controls and welders by education and BMI, but controls in the overall cohort had significantly more education and lower BMIs (Table 1; Lee et al., 2015). All welders underwent an orbital radiograph to rule out any metal fragments around the eye prior to brain MRI. Written informed consent was obtained from all subjects in accordance with the Declaration of Helsinki and

Table 1
Demographic, exposure, and MRI metrics for welders and controls.

	Controls (N = 13)	Welders (N = 20)	p-values
Age (years)	41.9 ± 10.8	47.1 ± 12.9	0.239
Education (years)	16.3 ± 2.0	13.3 ± 2.2	<0.001
ALT (IU/L)	37.1 ± 16.7	45.1 ± 19.9	0.240
BMI (kg/m^2)	25.1 ± 3.2	29.4 ± 5.9	0.020
HrsW (hours)	0 ± 0 (0)	162 ± 140	<0.001
YrsW (years)	0 ± 0 (0)	24.7 ± 12.3	<0.001
MRI metrics			
PI	108.9 ± 1.3	109.2 ± 1.8	0.436
R1			
Caudate	0.670 ± 0.058	0.676 ± 0.091	0.854
Putamen	0.712 ± 0.064	0.701 ± 0.046	0.552
Globus pallidus	0.889 ± 0.081	0.867 ± 0.039	0.161
R2*			
Caudate	21.5 ± 1.9	23.6 ± 3.0	0.080
Putamen	25.9 ± 2.7	27.2 ± 3.7	0.472
Globus pallidus	34.5 ± 5.4	37.8 ± 5.2	0.826
FA			
Caudate	0.166 ± 0.014	0.176 ± 0.018	0.220
Putamen	0.211 ± 0.029	0.237 ± 0.030	0.280
Globus pallidus	0.349 ± 0.034	0.358 ± 0.027	0.649
MD			
Caudate	7.80×10^{-4}	7.66×10^{-4}	0.110
Putamen	7.35×10^{-4}	7.45×10^{-4}	0.618
Globus pallidus	7.73×10^{-4}	7.58×10^{-4}	0.282

All data represent the mean ± SD, unless otherwise indicated. Data were analyzed using ANCOVA except for gender and handedness, which were analyzed using Fisher's Exact test. Abbreviations: ALT, alanine aminotransferase; BMI, body mass index; FA, fractional anisotropy; HrsW, hours welding in the 90 days prior to study visit; MD, mean diffusivity; PI, pallidal index; YrsW, total years welding.

approved by the PSHMC Internal Review Board/Human Subjects Protection Office.

2.1.1. Clinical information

All subjects were examined and ascertained to be free of any obvious neurological and movement deficits using the UPDRS motor scores (UPDRS-III) with a threshold score of <15 indicating lack of parkinsonian motor symptoms as defined by a previous welder study (Lee et al., 2015). Subjects also completed sections I (a non-motor-related functional questionnaire) and II (a motor-related functional questionnaire) of the UPDRS. None of the control subjects had any arthritis in their upper extremities. Descriptive data for all subjects are presented in Table 1.

2.2. Experimental design

All subjects were assigned a study identification number (study ID) upon enrollment. This study ID then was used during data analysis so that analyses could be carried out in a blinded fashion. Subjects were not randomly assigned to a group, as group assignment was dictated by previous welding history. A priori sample size calculations based on a power analysis using G*Power (Faul et al., 2007) suggested studying at least 11 control and 21 welders in order to achieve an effect size (d) greater than 1.1 with at least 80% power and type-I error rate of $\alpha = 0.05$ to detect a group difference. The effect size was estimated based on our previous study with 10 PD patients compared to 11 controls, which revealed a large effect size of d = 1.39 for the synergy index group difference [1.79 ± 0.49 for PD vs. 2.58 ± 0.64 for controls; (Park et al., 2012)]. The actual sample size of 13 controls and 20 welders would yield 85% power to detect the assumed effect size for a group difference.

2.3. Exposure assessment

Exposure first was assessed by the work history (WH) questionnaire that collected job information over the individual's working lifetime, emphasizing welding and other jobs associated with welding exposure. Responses on the WH enabled an estimate of cumulative lifetime years welding (YrsW). An additional supplementary exposure questionnaire (SEQ; Lee et al., 2015) focused on the 90-day period prior to the MRI and determined the time spent welding, type of metal welded, and various types of welding performed. The exposure metrics derived from the SEQ were: hours welding, brazing, or soldering [HrsW = (weeks worked) * (h/week) * (fraction of time worked related directly to welding)] in the 90-day period preceding the MRI (Lee et al., 2015).

2.4. Apparatus

2.4.1. Multi-digit pressing setup

This setup has been described in more detail previously (Park et al., 2012). Briefly, four piezoelectric force sensors (model 208A03; PCB Piezotronics, Depew, NY) were used to measure vertical forces produced by the fingers. The sensors were attached to a customized flat wooden panel. Each sensor was covered with sandpaper (300-grit) to increase the friction between the fingertips and the top surface of the sensors. Sensor positions in the medial-lateral and anterior-posterior directions were adjusted according to individual hand and finger anatomy to achieve a comfortable hand posture. A wooden piece was placed underneath the subject's palm to help maintain constant hand and finger configurations during the tests (see schematic in Fig. 1). The four force signals were digitized at 300 Hz with a 16-bit resolution using a customized LabView program.

2.5. Experimental procedures

The experiment comprised three tasks: 1) maximal voluntary contraction (MVC) tasks, 2) single-finger ramp tasks, and 3) quick force pulse production tasks. The subjects performed all three tasks in the above order with their dominant (right) and non-dominant (left) hand. The entire experiment lasted ~1 h. Before each task, subjects were given instructions and a demonstration by an experimenter, after which they practiced for 1–3 min.

2.5.1. Pressing tasks

Subjects sat in a chair facing a 19-in. computer monitor positioned at eye level. The monitor showed real-time finger force feedback. The forearm was strapped into a wrist-forearm brace to avoid forearm and wrist movement during trials (see Fig. 1). Prior

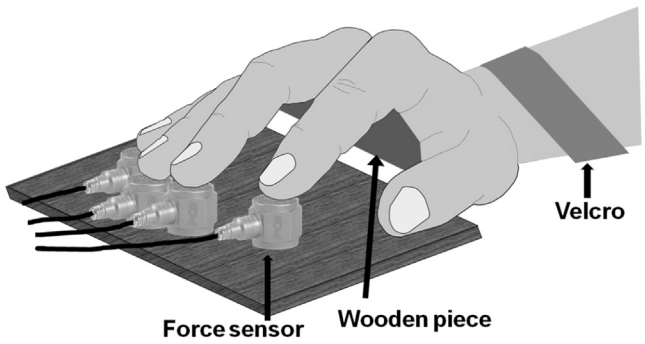

Fig. 1. Schematic of the pressing setup.

to each trial, all sensor signals were set to zero when subjects placed their fingertips on the sensor centers and relaxed their hand. As a result, the sensors measured only active downward forces.

2.5.1.1. MVC task. In the MVC task, subjects were instructed to press on the sensors with the four fingers together as hard as possible in a self-paced manner and achieve maximal total force level within 8 s. Subjects were instructed to relax immediately after reaching a maximal force. The feedback showed the sum of the four finger forces (F_{TOT}). Maximal total force (MVC_{TOT}) and the forces of individual fingers (MVC_i; i = I, index; M, middle; R, ring; and L, little) were measured. Subjects performed two consecutive attempts, and the trial with the higher MVC_{TOT} was selected to set further tasks with the pressing setup.

2.5.1.2. Single-finger ramp tasks. Subjects were required to press with one of the fingers (the task finger) and match its force with the template shown on the screen. The 20-s template consisted of a horizontal segment at zero force for the first 4 s, followed by a slanted line from 0% to 40% of the force of the task finger measured in the MVC test over the next 12 s, and a horizontal segment at 40% of MVC_i for the last 4 s. Subjects were asked to pay no attention to possible force production by other fingers (non-task fingers) and to keep all fingers on the sensors at all times.

2.5.1.3. Accurate multi-finger force pulse production task. In this task, subjects were asked to produce an accurate steady-state force level followed by a quick force pulse into a target by pressing with all four fingers. During each trial, the feedback on F_{TOT} was provided on the computer screen. Two horizontal lines showed an initial force level (set at 5% of MVC_{TOT}) and a target level (set at 25% of MVC_{TOT}; with ±5% error margins). The instruction was to press on the sensors with all four fingers and match F_{TOT} with the initial force level as accurately as possible. A vertical line was shown corresponding to 5 s after the trial initiation. Once the cursor crossed the vertical line, the subjects were required to produce a very quick force pulse to the target at a self-selected time within the next 5 s. Each subject performed at least 25 trials and additional trials (over the minimum 25) were given if the subject made a major mistake (for example, pressing before the cursor reached the vertical line, pressing several times within 1 trial, or changing the baseline force slowly in preparation to pressing).

2.5.2. Grooved Pegboard Test

The *Grooved Pegboard Test* (Lafayette Instrument Company, Lafayette, Indiana) is a conventional neurobehavioral assessment to measure fine motor dexterity and used widely in patient populations (reviewed in Causby et al., 2014). This test contains 25 holes with randomly positioned slots and pegs that have a key along one side. Subjects were asked to rotate the pegs to match the hole before it could be inserted. Subjects were instructed to place all pegs into the 25 holes, picking them up one at a time, and using just one hand. They completed the test first using their dominant and then their non-dominant hand. Total completion time was measured using a stopwatch. Average scores for the dominant or non-dominant hands in each group were calculated. The scores then were transformed to z-scores based on age- and education-adjusted norm scores (Ruff and Parker, 1993).

2.5.3. MRI data acquisition

All images were acquired using a Siemens 3 T scanner (Magnetom Trio, Siemens Medical Solutions, Erlangen, Germany) with an 8-channel head coil. High-resolution T1-weighted (T1W) and T2-weighted (T2W) images were acquired for anatomical segmentation. T1W images were collected using an MPRAGE sequence with Repetition Time (TR) = 1540 ms, Echo Time (TE) = 2.3 ms, FoV = 256 × 256 mm, matrix = 256 × 256 mm, slice thickness = 1 mm, slice number = 176 (with no gap), and voxel spacing 1 × 1 × 1 mm. T2W images were acquired using a fast-spin-echo sequence with TR/TE = 2500/316, and the same spatial resolution as the T1W images.

For whole brain fast T1 mapping, images were acquired using a spoiled gradient recalled echo (SPGR) with two flip angles and transmit field (B1) correction. Image acquisition parameters for the T1 mapping were as follows: TR = 15 ms, TE = 1.45 ms, flip angles = 4/25, FoV = 250 × 250 mm, matrix = 160 × 60, slice thickness = 1 mm, slice number = 192 50% overlap, and voxel spacing = 1.56 × 1.56 × 1 mm; and for the B1 field mapping: TR = 1000 ms, TE = 14 ms, flip angles = 45/60/90/120/135, FoV = 250 × 250 mm, matrix = 32 × 32, slice thickness = 5 mm, and slice number = 22.

For R2*, five echoes with TE ranging from 8 to 40 ms and an interval of 8 ms were acquired with TR = 51 ms, flip angle = 15°, FoV = 230 mm × 230 mm, matrix = 256 × 256, slice thickness = 1.6 mm, and slice number = 88. For R1, parameters were TR = 15 ms, TE = 1.45 ms, flip angles = 4/25, FoV = 250 × 250 mm, matrix = 160 × 160, slice thickness = 1 mm, slice number = 192, and voxel spacing = 1.56 × 1.56 × 1 mm.

For DTI, TR/TE = 8300/82 ms, b value = 1000 s/mm^2, diffusion gradient directions = 42 and 7 b = 0 scans, FoV = 256 × 256 mm, matrix = 128 × 128, slice thickness = 2 mm (with no gap), and slice number = 65 were used.

2.6. Data analysis

2.6.1. Finger force data

The force data were digitally low-pass filtered with a zero-lag, fourth-order Butterworth filter at 10 Hz. The data processing was done using a customized Matlab code as described previously (Jo et al., 2015). For each subject and each hand, we computed maximum voluntary force (MVC_{TOT}) in the *MVC* trials, the time to peak force during the quick force-pulse production trials (t_{Ftot}), and an overall index of enslaving (*EN*) in the single-finger ramp tasks. Enslaving is unintentional force production by non-task fingers when one of the fingers (task finger) produces force intentionally (Zatsiorsky et al., 2000). To compute the index of enslaving, for each single-finger trial, linear regressions of the force produced by individual fingers against F_{TOT} over a 10-s time interval were computed. The first and last 1-s intervals were excluded to avoid edge effects. The regression coefficients in $F_{i,j} = f_i^0 + k_{i,j} \times F_{TOT,j}$ were used to construct:

$$E = \begin{bmatrix} k_{I,I} & k_{I,M} & k_{I,R} & k_{I,L} \\ k_{M,I} & k_{M,M} & k_{M,R} & k_{M,L} \\ k_{R,I} & k_{R,M} & k_{R,R} & k_{R,L} \\ k_{L,I} & k_{L,M} & k_{L,R} & k_{L,L} \end{bmatrix}$$

Where i, j = {I, M, R, L}; j represents a task finger; $F_{i,j}$ and $F_{TOT,j}$ indicate the individual i-finger force and F_{TOT}, respectively, when j-finger was the task-finger. An overall index of enslaving, EN_j, was computed for each finger as the average $k_{i,j}$ across the non-task fingers when j-finger was the task-finger: $EN_j = \sum k_{i,j}/3$ ($i \neq j$).

We calculated synergy indices for each hand within the framework of the UCM hypothesis (Scholz and Schoner, 1999; Latash et al., 2001). Finger forces were transformed into finger modes (**m**) with the help of the **E** matrix. Mode is a hypothetical neural variable reflecting the intentional force production by a finger leading to forces by all the fingers of the hand due to enslaving. The variance in the mode space across all the accepted trials was quantified separately in two sub-spaces for each time sample. The first sub-space (UCM) corresponded to no changes in

F_{TOT}. The second sub-space was the orthogonal complement (ORT) to the UCM; variance within ORT changed F_{TOT}. The two variance components (V_{UCM} and V_{ORT}) were further combined into a single metric, a synergy index, ΔV, which was computed for each time sample: $\Delta V = (V_{UCM} - V_{ORT})/V_{TOT}$, where each variance index is normalized by the number of degrees-of-freedom in the corresponding spaces, 3 for UCM, 1 for ORT, and 4 for TOT; V_{TOT} stands for total variance.

We interpret $\Delta V > 0$ as sign of a F_{TOT} – stabilizing synergy; a higher ΔV implies a stronger synergy. For further statistical analysis, ΔV was log-transformed (ΔV_Z) using the Fischer transformation applied for the computational boundaries, from −4 to +1.333.

The time (t_0) of initiation of F_{TOT} change was defined as the time when the first derivative of force (dF/dt) reached 5% of its peak value in that particular trial. All the accepted trials for each hand and each subject were aligned with respect to t_0. The time to reach peak force (t_{Ftot}) was defined as the time of peak force with respect to t_0. The average value (ΔV_{SS}) and standard deviation (SD) of ΔV_Z were computed for the steady-state interval (between −600 and −400 ms prior to t_0).

Anticipatory synergy adjustment (ASA; see Fig. 2) was quantified using two indices, the difference in the ΔV_Z between steady state and t_0 ($\Delta\Delta V_Z$) and the time of initiation of the ΔV_Z drop (t_{ASA}). The t_{ASA} index was defined as the time when ΔV_Z dropped below its average steady-state value (ΔV_Z) by more than 2 SD. Negative values of t_{ASA} mean that ΔV_Z started to drop before the initiation of F_{TOT} changes.

2.6.2. Imaging data

2.6.2.1. Defining brain regions of interest. Bilateral basal ganglia structures (putamen, caudate, and globus pallidus) were defined for each subject using automatic segmentation software (AutoSeg; Joshi et al., 2004; Gouttard et al., 2007) as regions of interests (ROIs) and then eroded by 1 voxel using a morphological operation in order to ensure the segmented ROIs were within the anatomical ROIs based on the T1W image. The quality of the segmentation then was confirmed visually for all subjects by a reviewer blinded to group assignment. Bilateral ROIs were analyzed separately (please see Statistical analysis section below).

2.6.2.2. Estimations of brain MRI measurements.

R1 values: R1 values in each ROI were calculated as 1/T1 in each voxel and averaged over the entire ROI as previously described (Lee et al., 2015).

Pallidal index: The PI was derived from the ratio of globus pallidus T1W intensity to frontal white matter intensity [PI = (globus pallidus/FWM) × 100] (Krieger et al., 1995) as previously described (Lee et al., 2015).

R2* values: R2* values in each ROI were calculated as 1/T2* in each voxel and averaged over the entire ROI as previously described (Lee et al., 2016b).

DTI values: Two DTI values [fractional anisotropy (FA) and mean diffusivity (MD)] were calculated out of three diffusivity eigenvalues (λ1, λ2, λ3; Le Bihan et al., 2001). FA is a weighted average of pairwise differences of the three eigenvalues and may represent the degree of diffusion anisotropy.

$$FA = \sqrt{\frac{1}{2}}\frac{\sqrt{(\lambda_1-\lambda_2)^2+(\lambda_2-\lambda_3)^2+(\lambda_3-\lambda_1)^2}}{\sqrt{\lambda_1^2+\lambda_2^2+\lambda_3^2}}$$

MD is an average of the three eigenvalues and provides information regarding the magnitude of the diffusion (Le Bihan et al., 2001; Du et al., 2014; Lee et al., 2016a).

2.7. Statistical analysis

Group comparisons were conducted using one-way ANOVAs. For motor tasks of synergy data [*MVC, EN,* and outcome variables of the quick force pulse production task (t_{Ftot}, ΔV_{SS}, $\Delta\Delta V_Z$, and t_{ASA})] and Grooved Pegboard, analysis of covariance (ANCOVA) was used with adjustments for age and education level. For MRI DTI (FA and MD), R1, R2*, and PI data, ANCOVA was used with adjustments for age, body mass index (BMI), and respirator use.

Spearman partial correlation analyses were conducted between motor tasks that showed significant group differences and welding-related exposure measurements (exposure metrics and MRI markers) after adjusting for age in welders. The imaging data for one welder was excluded due to poor quality, resulting in 19 welders included in the imaging and correlation analyses.

Since there were several subtests for the synergy task and multiple basal ganglia regions for the MRI markers to be compared,

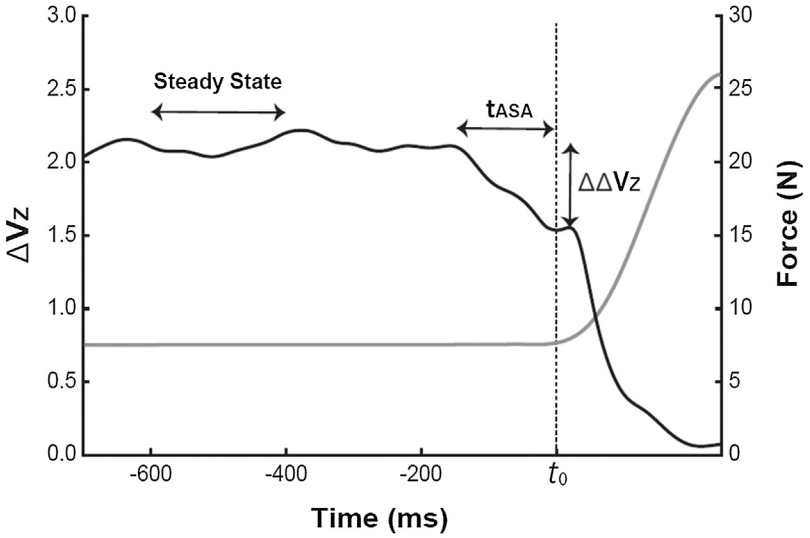

Fig. 2. Total force (gray line) and index of synergy (ΔV_Z, black line) during the force pulse production task by a representative welder subject. Note the drop in ΔV_Z starting prior to the force pulse initiation (t_0). The figure also shows the time (t_{ASA}) and magnitude ($\Delta\Delta V_Z$) of the anticipatory synergy adjustment.

the group comparisons of motor tasks (synergy data), MRI markers, and the correlation analyses were corrected for multiple comparisons using the Stepdown Bonferroni method (Holm, 1979) to control the familywise error rate (*FWER*) at $p = 0.05$. All statistical tests were two-tailed.

We reported raw p values and marked the values (*) that remain significant after correction for multiple comparisons. SAS 9.3 was used to perform all statistical analyses.

3. Results

3.1. Demographic

There were no group differences in age or ALT (a measure of liver function; Table 1). Control subjects had significantly more years of education than welders ($p < 0.001$). The BMI was significantly higher in welders compared to controls ($p = 0.020$).

3.1.1. Welding-related exposure

Exposure metrics: HrsW ($p < 0.001$) and YrsW ($p < 0.001$) measures were significantly higher in welders compared to controls (Table 1).

MRI markers: There were no group differences in any welding-related MRI markers in any ROI either using the combined or separate measures for each hemisphere after adjustment for age, BMI, and respirator use (ps > 0.079; Table 1). Significant group differences in welding-related MRI markers with a larger sample of the same cohort, however, have been reported previously (Lee et al., 2015, 2016a, 2016b).

3.2. Motor tasks

3.2.1. UPDRS and Grooved Pegboard scores

As seen in Table 2, there were no significant differences in the UPDRS total score or the motor (sections II and III) and non-motor (section I) sub-scores. There also were no significant differences between welders and controls on the Grooved Pegboard test (ps > 0.128; Table 2).

3.2.2. Maximal voluntary contraction (MVC) and enslaving (EN)

Maximal force values (*MVC*) produced by welders were similar to those produced by controls (ps > 0.05, Table 2). Both groups showed substantial force production by the non-task fingers during single-finger ramp force production tasks. The enslaving index (*EN*) in both groups was similar in each hand (Table 2). Time to peak force (t_{Ftot}) also did not differ between the groups (ps > 0.91).

3.2.3. Multi-finger synergies and ASA measures

All subjects showed much higher inter-trial variance of commands to fingers (force modes) compatible with an unchanged value of total force (V_{UCM}) compared to the variance that changed total force (V_{ORT}). This was reflected in consistently positive synergy indices quantified over the steady-state accurate force production, ΔV_{SS} (Table 2). Welders had a significantly lower steady-state synergy index (ΔV_{SS}) of the left hand compared to controls ($p = 0.004$, Table 2), which remained significant after correction for multiple comparisons, whereas the difference did not reach statistical significance in the right hand ($p = 0.160$). Thus, we focused on synergy indices on the left hand for the correlation analyses in the next section.

Table 2
Performance characteristics for motor measurements.

	Controls	Welders	P values
UPDRS subscores			
I	3.8 ± 3.3	4.5 ± 3.4	0.549
II	0.62 ± 1.4	0.80 ± 1.3	0.703
III	1.6 ± 2.8	2.7 ± 2.9	0.461
Total	6.0 ± 5.2	8.0 ± 4.8	0.278
Grooved Pegboard Tests			
Right hand	−0.127 ± 0.871	0.458 ± 1.300	0.135
Left hand	−0.189 ± 1.036	0.312 ± 1.270	0.183
Finger test measures			
Maximal voluntary contraction (N)			
Right hand	89.5 ± 31.9	86.2 ± 26.7	0.796
Left hand	90.0 ± 29.2	82.2 ± 27.2	0.698
Enslaving indices			
Right hand	0.690 ± 0.217	0.673 ± 0.222	0.658
Left hand	0.831 ± 0.402	0.700 ± 0.293	0.175
Time to peak force (s)			
Right hand	0.146 ± 0.023	0.146 ± 0.038	0.909
Left hand	0.141 ± 0.024	0.143 ± 0.035	0.940
Synergy measures			
Overall steady-state synergy index, ΔV_{SS}			
Right hand	2.257 ± 0.253	2.040 ± 0.425	0.160
Left hand	2.615 ± 0.392	2.213 ± 0.275	**0.004***
Time of anticipatory synergy adjustment (s)			
Right hand	−0.176 ± 0.140	−0.162 ± 0.118	0.692
Left hand	−0.152 ± 0.093	−0.187 ± 0.131	0.292
Synergy index change during ASA, $\Delta\Delta V_Z$			
Right hand	−0.475 ± 0.345	−0.407 ± 0.221	0.870
Left hand	−0.524 ± 0.336	−0.390 ± 0.237	0.231

Data represent the means ± the standard deviation (SD). For the Grooved Pegboard data are presented as the mean ± SD and represent the z-transformed time needed to complete the task. Data were analyzed using analysis of covariance (ANCOVA) with adjustment for age and education level. *Represents comparisons that survived adjustment for multiple comparisons. All the ΔV indices were log-transformed. Abbreviations: UPDRS, Unified Parkinson's Disease Rating Scale.

Prior to the force pulse initiation, both groups showed a consistent drop in ΔV, which started on average ~170 ms prior to the first detectable change in total force. Fig. 2 illustrates a typical performance by one of the welder subjects. Note the drop in the synergy index ΔV_Z (black line) prior to the time of force pulse initiation (t_0). The initiation time of the ΔV drop (t_{ASA}) and the change in the synergy index during ASA ($\Delta\Delta V_Z$) were not significantly different between the two groups in either hand (ps > 0.231; Table 2).

3.2.4. Synergy associations with exposure and imaging measures

Since the left steady-state synergy index (ΔV_{SSL}) was the only synergy metric showing a significant group difference, this metric was used in the exposure and imaging correlation analyses.

3.2.4.1. Exposure measurements. The synergy index of the left hand (ΔV_{SSL}) correlated negatively with HrsW (r = −0.477, p = 0.039) and YrsW at a trend level (r = −0.448, p = 0.055) in welders. The significant relationship between ΔV_{SSL} and HrsW, however, did not survive correction for multiple comparisons. Controls had no exposure measures to correlate.

3.2.4.2. R1, R2, and PI measurements.* There were no significant associations between the left synergy index (ΔV_{SSL}) and any of the MRI measurements for Mn (R1 or PI) or iron (R2*) accumulation in welders or controls (Supplemental Table 1).

3.2.4.3. FA and MD measurements. The synergy index of the left hand (ΔV_{SSL}) was correlated positively with FA values in the left globus pallidus in welders (r = 0.731, p = 0.0006, Fig. 3, Supplemental Table 1A), which remained significant after correction for multiple comparisons. The relationship was lacking in controls (Fig. 3, Supplemental Table 1B). ΔV_{SSL} also was correlated positively with FA values in the right caudate (r = 0.486, p = 0.041) in welders and negatively with the right putamen in controls (r = −0.667, p = 0.018), but neither association survived correction for multiple comparisons. ΔV_{SSL} was not correlated with MD values in any ROI for either welders or controls (ps > 0.068; Supplemental Table 1).

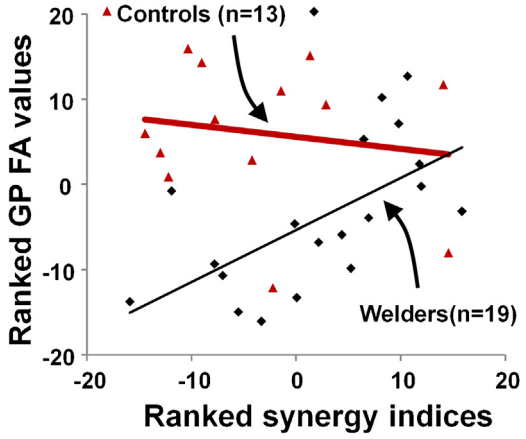

Fig. 3. Welders (black line) demonstrated a strong and significant correlation between the synergy index and GP FA values, whereas controls (red line) showed no significant relationship between the two measures. GP FA values and synergy indices were ranked due to non-normal distributions. (For interpretation of the references to colour in this figure legend, the reader is referred to the web version of this article.)

4. Discussion

This is the first study to examine whether multi-digit synergies may capture subclinical basal ganglia dysfunction in asymptomatic welders. The results confirmed the hypotheses formulated in the Introduction: 1) welders had a decreased synergy index compared to control subjects, particularly for the left hand; and 2) the synergy index was correlated with welding-related imaging metrics reflecting microstructural changes in the basal ganglia of welders. The results, however, do not support that synergy measurements correlated with measures of Mn or Fe metal accumulation per se. Together, these data suggest that multi-digit synergy metrics may serve as preclinical markers for basal ganglia dysfunction in welders and, potentially, other populations at risk for basal ganglia dysfunction. The findings may have important clinical, scientific, and public/occupational health implications as we discuss below.

4.1. Synergy studies as a tool to measure impaired motor stability in welders

A series of studies have shown that impaired control of action stability happens with healthy aging (Shinohara et al., 2004; Olafsdottir et al., 2007a,b). Those studies tested healthy elderly subjects (70–85 years of age) and documented a reduction in the synergy index in multi-digit pressing and prehensile tasks. Two studies have shown that exercise may lead to a significant improvement in the synergy index in older adults (Olafsdottir et al., 2008; Wu and Hallett, 2013). Recently, our group has demonstrated synergy changes in patients with basal ganglia dysfunction (PD and parkinsonism; Park et al., 2013b; Jo et al., 2015).

This study is the first to investigate multi-finger synergies in asymptomatic welders exposed to Mn, which at high levels is associated with Mn-induced parkinsonism. The finding of a decreased synergy index, a metric for movement stability, in asymptomatic welders is consistent with the involvement of the basal ganglia, which is vulnerable to welding-related damage due to higher metal accumulation (Kim et al., 1999; Dorman et al., 2006; Criswell et al., 2012; Lee et al., 2015, 2016b). In addition, this finding is consistent with previous literature that welders have issues with balance and tasks requiring maintaining stability (Mergler et al., 1994; Bouchard et al., 2007; Bowler et al., 2007c; Zoni et al., 2007; Ellingsen et al., 2008).

Welders generally hold a torch or electrode and repeat a very precise motion with their dominant (e.g., right) hand, while using their non-dominant (left) hand to guide and stabilize the object. Several recent studies have shown that multi-digit synergies are stronger in the non-dominant hand during steady-state tasks (Park et al., 2012; Jo et al., 2015). This observation fits well with the dynamic dominance hypothesis (Sainburg, 2002; Sainburg, 2014), which suggests that the non-dominant hand has an advantage during positional tasks. Indeed, the demonstrated advantage of the left hand in positional, steady-state tasks may be partly due to the higher stability in those tasks performed by the non-dominant hand. We observed significant group differences in the left hand synergy index during steady-state accurate force production, whereas the differences did not reach statistical significance in the dominant right hand. This is an intriguing result. Asymptomatic active welders are able to remain in their regular welding job that requires tremendous accuracy and agility (Ellingsen et al., 2008; Baker et al., 2015). In fact, welders may have superior motor function, especially in their dominant hand, compared to other manual workers not exposed to welding fumes, and be able to mask subtle welding-induced changes in motor functions when the exposure level is relatively low ("skilled-worker" phenomena).

This may have contributed to the lack of significant motor deficits in the dominant hand. Nevertheless, we did observe a trend in the right hand and increasing the sample size might reveal this difference. It would be interesting in future studies to obtain synergy metrics for tasks not involving hands, such as postural tasks, that may help test effector-specific vs. systemic effects on motor stability.

4.2. Synergy as a sensitive marker of basal ganglia dysfunction

As we discussed in the Introduction, the Grooved Pegboard has been used for gauging fine motor dysfunction (reviewed in Ruff and Parker, 1993; Causby et al., 2014). The sensitivity and usefulness of this test has been demonstrated in patient populations (Lee et al., 2013) but it may not be accurate in detecting subtle motor functional changes in subclinical populations (Ellingsen et al., 2008). Consistent with this notion, the pegboard test in the current study failed to detect significant differences between the groups, whereas the multi-finger synergy index succeeded in detecting these differences.

Several recent studies from our group have shown that impaired motor synergies during multi-finger action may be one of the earliest detectable motor dysfunctions in PD, even in the apparently unaffected (subclinical) side (Park et al., 2012, 2013a, 2014). Welders tested in the current study had no parkinsonian signs. In addition, their fine motor skills were comparable with those of controls and they showed no difference from controls in the ability to perform quick force pulses. The fact that we captured reduced synergy indices in this group of welders is consistent with the hypothesis that synergy changes may provide the earliest behavioral markers for basal ganglia dysfunction.

The synergy index is more specific to subcortical dysfunction and relatively preserved in cortical dysfunction (Reisman and Scholz, 2003; Reisman and Scholz, 2006; Jo et al., 2016), whereas ASA changes have been observed in both PD and cortical stroke patients (Jo et al., 2016). It is interesting to note that our welders showed reduced synergy indices during steady-state tasks, whereas the ASAs were unchanged. This result suggests that synergy index changes during steady-state tasks may be specific to subclinical changes in the basal ganglia while ASA changes may emerge later in progressive disorders when more diffuse neural networks are involved. It would be very interesting in future studies to see if ASA change occurs in clinical, symptomatic welders (manganism) and can be used to gauge the extent and severity of the associated neurodegenerative process.

4.3. Biological relevance of synergy-brain microstructural associations in understanding Mn-related neurotoxicity

Overt Mn neurotoxicity is known to have similarities to PD (Cersosimo and Koller, 2006; Bowler et al., 2007a). The neurotoxic effects of chronic and lower-level Mn exposure, at the level most relevant to occupational and public health, however, are less clear. Past studies of “asymptomatic” welders support an association between exposure to Mn-containing welding fumes and subclinical neural deficits (Ellingsen et al., 2008; Chang et al., 2009), but the conclusion was marred by the lack of an objective in vivo marker(s) to sensitively reflect Mn at the brain tissue level, the absence of accounting for co-exposed metal (i.e., iron) accumulation in brain tissue, and little investigation of their structural and functional consequences. In the current study, we leveraged the most recent advances in MRI to reflect basal ganglia metal (Mn and iron) accumulation and microstructural changes to address this gap.

The synergy index was not correlated with the metrics for Mn accumulation (R1 and the PI). This is not surprising because although these metrics (R1 and PI) may reflect sensitively current or ongoing brain Mn exposure, they may not capture long-term lingering effects of Mn on brain tissues or function, particularly when the levels of exposure are low (Han et al., 2008; Baker et al., 2015; Lee et al., 2016b).

The finding of a strong and significant association between the synergy index and globus pallidus FA values, the region known to have highest susceptibility for Mn accumulation, is very encouraging and suggests that the decline in motor stability is not only measurable, but also related to Mn-induced microstructural changes in the globus pallidus (Lee et al., 2016a). Indeed, in a previous study we found reduced globus pallidus FA values in asymptomatic welders that were robustly associated with the PI (a traditional measure for Mn accumulation in the globus pallidus; Lee et al., 2016a) but not with R2* values (Lee et al., 2016b). In contrast to MRI metrics for Mn accumulation that may be more sensitive to short-term dynamics of Mn-exposure, Mn-induced microstructural changes probably are related more to long-term, cumulative neurotoxic effects resulting from multiple transient exposures. In line with this notion, we recently discovered that globus pallidus FA changes, not Mn brain accumulation (particularly R1), are correlated with long-term Mn exposure metrics (Lee et al., 2016a).

4.4. Hemispheric control of motor function

Although motor function primarily is controlled by the contralateral hemisphere, previous work demonstrated significant and important ipsilateral hemisphere involvement in unimanual hand tasks (Davare et al., 2007), particularly when the task is complex (Singh et al., 1998; Haaland et al., 2004) or requires increased force (Hess et al., 1986; Muellbacher et al., 2000). Ipsilateral control of motor function is most evident in the left (dominant) hemisphere, as right-handed subjects more strongly activate the left motor cortex during left-handed tasks than the right motor cortex during right-handed tasks (Kim et al., 1993; Kobayashi et al., 2003). Virtual lesion studies confirm these imaging findings (Chen et al., 1997). Patients with stroke often have contralateral hemiparesis (Bourbonnais and Vanden Noven, 1989; Levin, 1996) but motor deficits ipsilateral to the lesion also are observed (Haaland and Harrington, 1996; Sunderland, 2000). Our finding of the strong relationship between left hand synergies and FA values in the left globus pallidus support important ipsilateral control in motor tasks. In addition, the association may reflect left (dominant) hemisphere specialization on multi-finger synergies to ensure stability of motor performance. Whereas the Spearman correlation between the right hand synergy index and left globus pallidus FA values was under the level of significance, testing a larger cohort and/or following subjects over time may clarify the relationship. Further studies are warranted to confirm these findings and elucidate the underlying mechanisms.

4.5. Limitations and summary

Although the results reported are intriguing and robust, the sample size is relatively small. The findings need to be replicated in a larger cohort, preferably with a longitudinal component, to determine whether these changes persist or evolve, and tasks not involving hands need to be tested to sort out effector vs. systemic effects. Nevertheless, our data suggested that the multi-digit synergy index can capture early and subclinical motor changes in asymptomatic welders and may serve as a preclinical marker for basal ganglia dysfunction in welders and other populations at risk for basal ganglia dysfunction.

Funding

XH, MML, GD, LK, and E-YL were supported by NIH grants ES019672 and NS082151 during the past 12 months. MLL and HJJ were supported by NIH grants NS035032 and AR048563.

Acknowledgments

We would like to thank all of the volunteers who participated in this study. In addition, we are indebted to many individuals who helped make this study possible, including: Melissa Santos and Susan Kocher for subject coordination, recruitment, blood sample handling, and data entry; Pam Susi and Pete Stafford of CPWR; Mark Garrett, John Clark, and Joe Jacoby of the International Brotherhood of Boilermakers; Fred Cosenza and all members of the Safety Committee for the Philadelphia Building and Construction Trades Council; Ed McGehean of the Steamfitters Local Union 420; Jim Stewart of the Operating Engineers; Sean Gerie of the Brotherhood of Maintenance of Way Employees Division Teamsters Rail Conference; and Terry Peck of Local 520 Plumbers, Pipefitters and HVAC.

Appendix A. Supplementary data

Supplementary data associated with this article can be found, in the online version, at http://dx.doi.org/10.1016/j.neuro.2016.06.016.

References

Baker, M.G., Criswell, S.R., Racette, B.A., Simpson, C.D., Sheppard, L., Checkoway, H., et al., 2015. Neurological outcomes associated with low-level manganese exposure in an inception cohort of asymptomatic welding trainees. Scand. J. Work Environ. Health 41 (1), 94–101.

Bouchard, M., Mergler, D., Baldwin, M., Panisset, M., Bowler, R., Roels, H.A., 2007. Neurobehavioral functioning after cessation of manganese exposure: a follow-up after 14 years. Am. J. Ind. Med. 50 (11), 831–840.

Bourbonnais, D., Vanden Noven, S., 1989. Weakness in patients with hemiparesis. Am. J. Occup. Ther. 43 (5), 313–319.

Bowler, R.M., Gysens, S., Diamond, E., Nakagawa, S., Drezgic, M., Roels, H.A., 2006a. Manganese exposure: neuropsychological and neurological symptoms and effects in welders. Neurotoxicology 27 (3), 315–326.

Bowler, R.M., Koller, W., Schulz, P.E., 2006b. Parkinsonism due to manganism in a welder: neurological and neuropsychological sequelae. Neurotoxicology 27 (3), 327–332.

Bowler, R.M., Nakagawa, S., Drezgic, M., Roels, H.A., Park, R.M., Diamond, E., 2007a. Sequelae of fume exposure in confined space welding: a neurological and neuropsychological case series. Neurotoxicology 28 (2), 298–311.

Bowler, R.M., Roels, H.A., Nakagawa, S., Drezgic, M., Diamond, E., Park, R., 2007b. Dose-effect relationships between manganese exposure and neurological, neuropsychological and pulmonary function in confined space bridge welders. Occup. Environ. Med. 64 (3), 167–177.

Bowler, R.M., Roels, H.A., Nakagawa, S., Drezgic, M., Diamond, E., Park, R., 2007c. Dose-effect relationships between manganese exposure and neurological, neuropsychological and pulmonary function in confined space bridge welders. Occup. Environ. Med. 64 (3), 167–177.

Causby, R., Reed, L., McDonnell, M., Hillier, S., 2014. Use of objective psychomotor tests in health professionals. Percept. Mot. Skills 118 (3), 765–804.

Cersosimo, M.G., Koller, W.C., 2006. The diagnosis of manganese-induced parkinsonism. Neurotoxicology 27 (3), 340–346.

Chang, Y., Kim, Y., Woo, S.T., Song, H.J., Kim, S.H., Lee, H., 2009. High signal intensity on magnetic resonance imaging is a better predictor of neurobehavioral performances than blood manganese in asymptomatic welders. Neurotoxicology 30 (4), 555–563.

Chen, R., Gerloff, C., Hallett, M., Cohen, L.G., 1997. Involvement of the ipsilateral motor cortex in finger movements of different complexities. Ann. Neurol. 41 (2), 247–254.

Cowan, D.M., Fan, Q., Zou, Y., Shi, X., Chen, J., Aschner, M., 2009a. Manganese exposure among smelting workers: blood manganese-iron ratio as a novel tool for manganese exposure assessment. Biomarkers 14 (1), 3–16.

Cowan, D.M., Zheng, W., Zou, Y., Shi, X., Chen, J., Rosenthal, F.S., 2009b. Manganese exposure among smelting workers: relationship between blood manganese-iron ratio and early onset neurobehavioral alterations. Neurotoxicology 30 (6), 1214–1222.

Criswell, S.R., Perlmutter, J.S., Huang, J.L., Golchin, N., Flores, H.P., Hobson, A., et al., 2012. Basal ganglia intensity indices and diffusion weighted imaging in manganese-exposed welders. Occup. Environ. Med. oemed-2011-100119.

Davare, M., Duque, J., Vandermeeren, Y., Thonnard, J.L., Olivier, E., 2007. Role of the ipsilateral primary motor cortex in controlling the timing of hand muscle recruitment. Cereb. Cortex 17 (2), 353–362.

Dorman, D.C., Struve, M.F., Marshall, M.W., Parkinson, C.U., James, R.A., Wong, B.A., 2006. Tissue manganese concentrations in young male rhesus monkeys following subchronic manganese sulfate inhalation. Toxicol. Sci. 92 (1), 201–210.

Du, G., Lewis, M.M., Sterling, N.W., Kong, L., Chen, H., Mailman, R.B., 2014. Microstructural changes in the substantia nigra of asymptomatic agricultural workers. Neurotoxicol. Teratol. 41, 60–64.

Eisen, A., Kiernan, M., Mitsumoto, H., Swash, M., 2014. Amyotrophic lateral sclerosis: a long preclinical period? J. Neurol. Neurosurg. Psychiatry 85 (11), 1232–1238.

Ellingsen, D.G., Konstantinov, R., Bast-Pettersen, R., Merkurjeva, L., Chashchin, M., Thomassen, Y., 2008. A neurobehavioral study of current and former welders exposed to manganese. Neurotoxicology 29 (1), 48–59.

Faul, F., Erdfelder, E., Lang, A.G., Buchner, A., 2007. G*Power 3: a flexible statistical power analysis program for the social, behavioral, and biomedical sciences. Behav. Res. Methods 39 (2), 175–191.

Gelfand, I.M., Latash, M.L., 1998. On the problem of adequate language in motor control. Motor Control 2 (4), 306–313.

Gouttard, S., Styner, M., Joshi, S., Smith, R.G., Hazlett, H.C., Gerig, G., 2007. Subcortical structure segmentation using probabilistic atlas priors. Medical Imaging; 2007. International Society for Optics and Photonics 65122J-J-11.

Guilarte, T.R., 2013. Manganese neurotoxicity: new perspectives from behavioral, neuroimaging, and neuropathological studies in humans and non-human primates. Front Aging Neurosci. 5, 23.

Haaland, K.Y., Harrington, D.L., 1996. Hemispheric asymmetry of movement. Curr. Opin. Neurobiol. 6 (6), 796–800.

Haaland, K.Y., Elsinger, C.L., Mayer, A.R., Durgerian, S., Rao, S.M., 2004. Motor sequence complexity and performing hand produce differential patterns of hemispheric lateralization. J. Cogn. Neurosci. 16 (4), 621–636.

Han, J.H., Chung, Y.H., Park, J.D., Kim, C.Y., Yang, S.O., Khang, H.S., 2008. Recovery from welding-fume-exposure-induced MRI T1 signal intensities after cessation of welding-fume exposure in brains of cynomolgus monkeys. Inhal. Toxicol. 20 (12), 1075–1083.

Hauser, R.A., Zesiewicz, T.A., Martinez, C., Rosemurgy, A.S., Olanow, C., 1996. Blood manganese correlates with brain magnetic resonance imaging changes in patients with liver disease. Can. J. Neurol. Sci. 23 (2), 95–98.

Hess, C.W., Mills, K.R., Murray, N.M., 1986. Magnetic stimulation of the human brain: facilitation of motor responses by voluntary contraction of ipsilateral and contralateral muscles with additional observations on an amputee. Neurosci. Lett. 71 (2), 235–240.

Holm, S., 1979. A simple sequentially rejective multiple test procedure. Scand. J. Stat. 65–70.

Huang, C.C., Lu, C.S., Chu, N.S., Hochberg, F., Lilienfeld, D., Olanow, W., 1993. Progression after chronic manganese exposure. Neurology 43 (8), 1479–1483.

Jo, H.J., Park, J., Lewis, M.M., Huang, X., Latash, M.L., 2015. Prehension synergies and hand function in early-stage Parkinson's disease. Exp. Brain Res. 233 (2), 425–440.

Jo, H.J., Maenza, C., Good, D.C., Huang, X., Park, J., Sainburg, R.L., 2016. Effects of unilateral stroke on multi-finger synergies and their feed-forward adjustments. Neuroscience 319, 194–205.

Joshi, S., Davis, B., Jomier, M., Gerig, G., 2004. Unbiased diffeomorphic atlas construction for computational anatomy. NeuroImage 23 (Suppl. 1), S151–60.

Kim, S.G., Ashe, J., Georgopoulos, A.P., Merkle, H., Ellermann, J.M., Menon, R.S., 1993. Functional imaging of human motor cortex at high magnetic field. J. Neurophysiol. 69 (1), 297–302.

Kim, S.H., Chang, K.H., Chi, J.G., Cheong, H.K., Kim, J.Y., Kim, Y.M., 1999. Sequential change of MR signal intensity of the brain after manganese administration in rabbits: Correlation with manganese concentration and histopathologic findings. Invest. Radiol. 34 (6), 383–393.

Kobayashi, M., Hutchinson, S., Schlaug, G., Pascual-Leone, A., 2003. Ipsilateral motor cortex activation on functional magnetic resonance imaging during unilateral hand movements is related to interhemispheric interactions. Neuroimage 20 (4), 2259–2270.

Krieger, D., Krieger, S., Theilmann, L., Jansen, O., Gass, P., Lichtnecker, H., 1995. Manganese and chronic hepatic encephalopathy. Lancet 346 (8970), 270–274.

Latash, M.L., Huang, X., 2015. Neural control of movement stability: Lessons from studies of neurological patients. Neuroscience 301, 39–48.

Latash, M.L., Scholz, J.F., Danion, F., Schoner, G., 2001. Structure of motor variability in marginally redundant multifinger force production tasks. Exp. Brain Res. 141 (2), 153–165.

Latash, M.L., Scholz, J.P., Schoner, G., 2002. Motor control strategies revealed in the structure of motor variability. Exerc. Sport Sci. Rev. 30 (1), 26–31.

Latash, M.L., Scholz, J.P., Schoner, G., 2007. Toward a new theory of motor synergies. Motor Control 11 (3), 276–308.

Latash, M.L., 2012. The bliss (not the problem) of motor abundance (not redundancy). Exp. Brain Res. 217 (1), 1–5.

Le Bihan, D., Mangin, J.F., Poupon, C., Clark, C.A., Pappata, S., Molko, N., 2001. Diffusion tensor imaging: concepts and applications. J. Magn. Reson. Imaging 13 (4), 534–546.

Lee, E.Y., Sen, S., Eslinger, P.J., Wagner, D., Shaffer, M.L., Kong, L., 2013. Early cortical gray matter loss and cognitive correlates in non-demented Parkinson's patients. Parkinsonism Relat. Disord. 19 (12), 1088–1093.
Lee, E.Y., Flynn, M.R., Du, G., Lewis, M.M., Fry, R., Herring, A.H., 2015. T1 relaxation rate (R1) indicates nonlinear Mn accumulation in brain tissue of welders with low-Level exposure. Toxicol. Sci. 146 (2), 281–289.
Lee, E.Y., Flynn, M.R., Du, G., Lewis, M.M., Herring, A.H., Van Buren, E., et al., 2016a. Lower fractional anisotropy in globus pallidus of asymptomatic welders, a marker for long-term welding exposure. Toxicol. Sci. 150 (2), 369–377.
Lee, E.Y., Flynn, M.R., Du, G., Li, Y., Lewis, M.M., Herring, A.H., et al., 2016b. Increased R2* in the caudate nucleus of asymptomatic welders. Toxicol. Sci..
Levin, M.F., 1996. Interjoint coordination during pointing movements is disrupted in spastic hemiparesis. Brain 119 (Pt. 1), 281–293.
Mandel, S.A., Korczyn, A.D., 2011. Biomarkers for prediction and targeted prevention of Alzheimer's and Parkinson's diseases: Evaluation of drug clinical efficact. EPMA J. 2 (Suppl. 1), 143–150.
Mergler, D., Baldwin, M., 1997. Early manifestations of manganese neurotoxicity in humans: an update. Environ. Res. 73 (1–2), 92–100.
Mergler, D., Huel, G., Bowler, R., Iregren, A., Belanger, S., Baldwin, M., 1994. Nervous system dysfunction among workers with long-term exposure to manganese. Environ. Res. 64 (2), 151–180.
Muellbacher, W., Facchini, S., Boroojerdi, B., Hallett, M., 2000. Changes in motor cortex excitability during ipsilateral hand muscle activation in humans. Clin. Neurophysiol. 111 (2), 344–349.
Olafsdottir, H., Yoshida, N., Zatsiorsky, V.M., Latash, M.L., 2005. Anticipatory covariation of finger forces during self-paced and reaction time force production. Neurosci. Lett. 381 (1–2), 92–96.
Olafsdottir, H., Yoshida, N., Zatsiorsky, V.M., Latash, M.L., 2007a. Elderly show decreased adjustments of motor synergies in preparation to action. Clin. Biomech. (Bristol, Avon) 22 (1), 44–51.
Olafsdottir, H., Zhang, W., Zatsiorsky, V.M., Latash, M.L., 2007b. Age-related changes in multifinger synergies in accurate moment of force production tasks. J. Appl. Physiol. 102 (4), 1490–1501.
Olafsdottir, H.B., Zatsiorsky, V.M., Latash, M.L., 2008. The effects of strength training on finger strength and hand dexterity in healthy elderly individuals. J. Appl. Physiol. 105 (4), 1166–1178.
Ostiguy, C., Asselin, P., Malo, S., 2006. The emergence of manganese-related health problems in Quebec: an integrated approach to evaluation, diagnosis, management and control. Neurotoxicology 27 (3), 350–356.
Pal, P.K., Samii, A., Calne, D.B., 1999. Manganese neurotoxicity: a review of clinical features, imaging and pathology. Neurotoxicology 20 (2–3), 227–238.
Park, J., Wu, Y.H., Lewis, M.M., Huang, X., Latash, M.L., 2012. Changes in multifinger interaction and coordination in Parkinson's disease. J. Neurophysiol. 108 (3), 915–924.
Park, J., Jo, H.J., Lewis, M.M., Huang, X., Latash, M.L., 2013a. Effects of Parkinson's disease on optimization and structure of variance in multi-finger tasks. Exp. Brain Res. 231 (1), 51–63.
Park, J., Lewis, M.M., Huang, X., Latash, M.L., 2013b. Effects of olivo-ponto-cerebellar atrophy (OPCA) on finger interaction and coordination. Clin. Neurophysiol. 124 (5), 991–998.
Park, J., Lewis, M.M., Huang, X., Latash, M.L., 2014. Dopaminergic modulation of motor coordinaton in Parkinson's disease. Parkinsonism Relat. Disord. 20 (1), 64–68.
Reisman, D.S., Scholz, J.P., 2003. Aspects of joint coordination are preserved during pointing in persons with post-stroke hemiparesis. Brain 126 (Pt. 11), 2510–2527.
Reisman, D.S., Scholz, J.P., 2006. Workspace location influences joint coordination during reaching in post-stroke hemiparesis. Exp. Brain Res. 170 (2), 265–276.
Ruff, R.M., Parker, S.B., 1993. Gender- and age-specific changes in motor speed and eye-hand coordination in adults: normative values for the Finger Tapping and Grooved Pegboard Tests. Percept. Mot. Skills 76 (3 Pt. 2), 1219–1230.
Sainburg, R.L., 2002. Evidence for a dynamic-dominance hypothesis of handedness. Exp. Brain Res. 142 (2), 241–258.
Sainburg, R.L., 2014. Convergent models of handedness and brain lateralization. Front. Psychol. 5, 1092.
Sandberg, G., Stewart, W., Smialek, J., Troncoso, J.C., 2001. The prevalence of the neuropathological lesions of Alzheimer's disease is independent of race and gender. Neurobiol. Aging 22 (2), 169–175.
Schöner, G., 1995. Recent developments and problems in human movement science and their conceptual implications. Ecolog. Psychol. 8, 291–314.
Scholz, J.P., Schoner, G., 1999. The uncontrolled manifold concept: identifying control variables for a functional task. Exp. Brain Res. 126 (3), 289–306.
Shinohara, M., Scholz, J.P., Zatsiorsky, V.M., Latash, M.L., 2004. Finger interaction during accurate multi-finger force production tasks in young and elderly persons. Exp. Brain Res. 156 (3), 282–292.
Simon-Sanchez, J., Schulte, C., Bras, J.M., Sharma, M., Gibbs, J.R., Berg, D., 2009. Genome-wide association study reveals genetic risk underlying Parkinson's disease. Nat. Genet. 41 (12), 1308–1312.
Singh, L.N., Higano, S., Takahashi, S., Abe, Y., Sakamoto, M., Kurihara, N., et al. Functional, M.R., 1998. imaging of cortical activation of the cerebral hemispheres during motor tasks. AJNR 19 (2), 275–280.
Sunderland, A., 2000. Recovery of ipsilateral dexterity after stroke. Stroke 31 (2), 430–433.
Wu, T., Hallett, M., 2013. The cerebellum in Parkinson's disease. Brain 136 (Pt. 3), 696–709.
Zatsiorsky, V.M., Li, Z.M., Latash, M.L., 2000. Enslaving effects in multi-finger force production. Exp. Brain Res. 131 (2), 187–195.
Zoni, S., Albini, E., Lucchini, R., 2007. Neuropsychological testing for the assessment of manganese neurotoxicity: a review and a proposal. Am. J. Ind. Med. 50 (11), 812–830.